Microstructure evolution and mechanical properties of Co-Fe-Ni-Ti-V eutectic high entropy alloy

Rahul M R[1a], Reliance Jain[2a], Sumanta Samal[2b*], Gandham Phanikumar[1b]

1Department of Metallurgical and Materials Engineering, Indian Institute of Technology Madras,Chennai-600036, Tamil Nadu, India.

[2]Discipline of Metallurgy Engineering and Materials Science, Indian Institute of TechnologyIndore, Khandwa Road, Simrol, Indore-453552, Madhya Pradesh, India.

[1a]rahulmr1991@gmail.com, [1b]gphani@iitm.ac.in, [2a]phd1701105011@iiti.ac.in, [2b*]sumanta@iiti.ac.in

ISBN: 978-963-508-889-8
Solidification and Gravity VII
Miskolc-Lillafüred, Hungary
September 3-6, 2018

Keywords: Eutectic high entropy alloy (EHEA), Microstructure evolution, Phase equilibria, Pseudo-quasiperitectic reaction, Mechanical property.

Abstract:
The present study is aimed at understanding the sequence of phase evolution during solidification in $Co_{25}Fe_{25}Ni_{25}Ti_{20}V_5$eutectic high entropy alloys (EHEAs), synthesized byvacuum arc melting cum suction casting technique. The detailed X-ray diffraction (XRD) andelectron microscopic (SEM and TEM) coupled with energy dispersive spectroscopic (EDS)analyses reveal the presence of BCC (β), FCC_1 (α_1), FCC_2 (α_2) and Ni_3Ti phases. For Co-Fe-Ni-Ti-V HEA, at first Ni_3Ti (DO24) primary dendritic phase is formed from theliquid, followed by peritectic reaction to form FCC_1 (α_1) phase (i.e. Ni_3Ti + L⟶FCC_1(α_1)). Then the remaining liquid undergoes eutectic reaction to form FCC_1 (α_1) and FCC_2 (α_2)phases (i.e. coarse eutectic: L⟶FCC_1 (α_1) + FCC_2 (α_2)). Finally, the remaining liquidundergoes eutectic reaction to form BCC (β), and FCC_2 (α_2) (i.e. fineeutectic: L⟶BCC (β) + FCC_2 (α_2). Therefore, based upon sequence of microstructuralevolution, two pseudo-quasiperitectic reactions i.e. L+ Ni_3Ti → FCC_1 (α_1) + FCC_2 (α_2) and L+ FCC_1 (α_1) ⟶BCC (β) + FCC_2 (α_2) have been proposed for the investigated EHEA. It isalso found that $Co_{25}Fe_{25}Ni_{25}Ti_{20}V_5$EHEAs retains high strength at elevatedtemperature.

1. Introduction

The complex concentrated high entropy alloys (HEAs) [1-8] consisting multiple principal elements in equiatomic or near equiatomic ratio exhibits simple microstructure of FCC and/or BCC solid solution phase. This is attributed to the several importantcore effects in HEAs [4, 5] such as high configurational entropy, severe lattice distortion and sluggish diffusion [9. 10].Yeh et al. [1] first reported $CuCoNiCrAl_xFe$ HEAs which shows good strength at elevated temperature up to 500^{o}C. The refractory HEAs such as $Nb_{25}Mo_{25}Ta_{25}W_{25}$

and $V_{20}Nb_{20}Mo_{20}Ta_{20}W_{20}$alloys have been studied by Senkov et al. [11] which exhibits excellent mechanical properties at high temperatures. Similarly, new class ofmulticomponent eutectic HEAs[5, 12-14], exhibiting good high temperature strengthhave also been reportedin the open literature. Although a lot of new and exciting research work has been done by many research groups across globe in thefield of HEAs to designnovelmaterials for possible industrial applications by choosing elements and composition judiciously in order to obtainunique microstructural features. Therefore, an attempt is made in this direction to develop novel HEA with improved mechanical properties at elevated temperature.

The objective of the present study is to understand the sequence of phase evolution during solidification and to establish new phase equilibria based upon detailed microstructural characterization as well as to evaluate the high temperature mechanical properties in the newly designedmulticomponent $Co_{25}Fe_{25}Ni_{25}Ti_{20}V_5$ HEA.

2. Experimental materials and procedures

High purity commercial Co, Fe, Ni, Ti and Velementswere used as the starting materials to prepare$Co_{25}Fe_{25}Ni_{25}Ti_{20}V_5$ HEA (henceforth referred to as EHEA)by arc melting technique under ultra high purity argon gas to obtain arc melted alloy button. The structural characterization of studied high entropy alloy was carried by X-ray diffraction (XRD) (Panalytical X-pert pro instrument) with Cu-K_α (λ = 0.154056 nm) radiation, operating at 45 kV and 30 mA, with step size of 2θ = 0.017 deg. The peaks in the XRD pattern were identified using International Committee for Diffraction Data (ICDD) database in PCPDFWIN software. The microstructural characterization of the samples was examined using the scanning electron microscope (Inspect F) equipped with an energy-dispersive spectrometer (EDS).Isothermal hot compression tests of the cylindrical samples (ϕ = 6 mm and aspect ratio of 1.5:1) were carried out using Gleeble 3800® thermo mechanical simulator at deformation temperatures of 800^{o}C (1073 K) and 1000^{o}C (1273 K) with constant strain rates of 10^{-1}.

3. Results and Discussion

3.1. Thermodynamic simulation

The thermodynamic simulations (as shown in Figure 1) of studied multicomponent EHEA have been carried out to understand the phase evolution and predict the equilibrium solidification path using TCHEA database in ThermoCalc software.It is observed that there are six equilibrium phases such as Ni_3Ti_DO24, FCC_L12, FCC_L12≠2, BCC_B2≠2, C14_LAVES and LIQUID phases from liquidus temperature (~1101^{o}C) to 780^{o}C. It is to be noted that at first Ni_3Ti phase is formed from the liquid, followed by formation of both FCC_L12, FCC_L12≠2 phases and finally BCC_B2≠2 and C14_LAVES phases are formed in this temperature range.

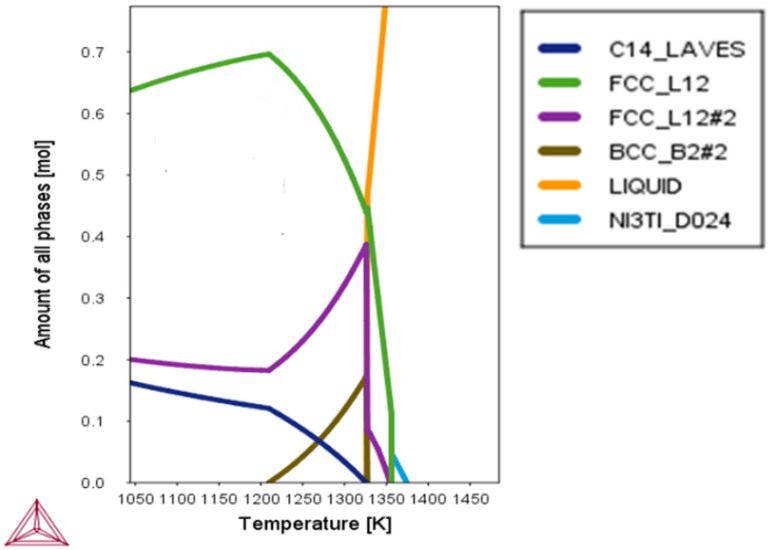

Figure 1: Thermodynamic simulation of multicomponent $Co_{25}Fe_{25}Ni_{25}Ti_{20}V_5$HEA.

3.2. Structural characterization

The XRD pattern of multicomponent EHEA is shown in Figure 2a. The XRD pattern shows the intense diffraction peaks corresponding to BCC solid solution phase (β), Disorder FCC1 solid solution phase (α_1), Order FCC2(L12) solid solution phase (α_2) and ordered Ni_3Ti_DO24.

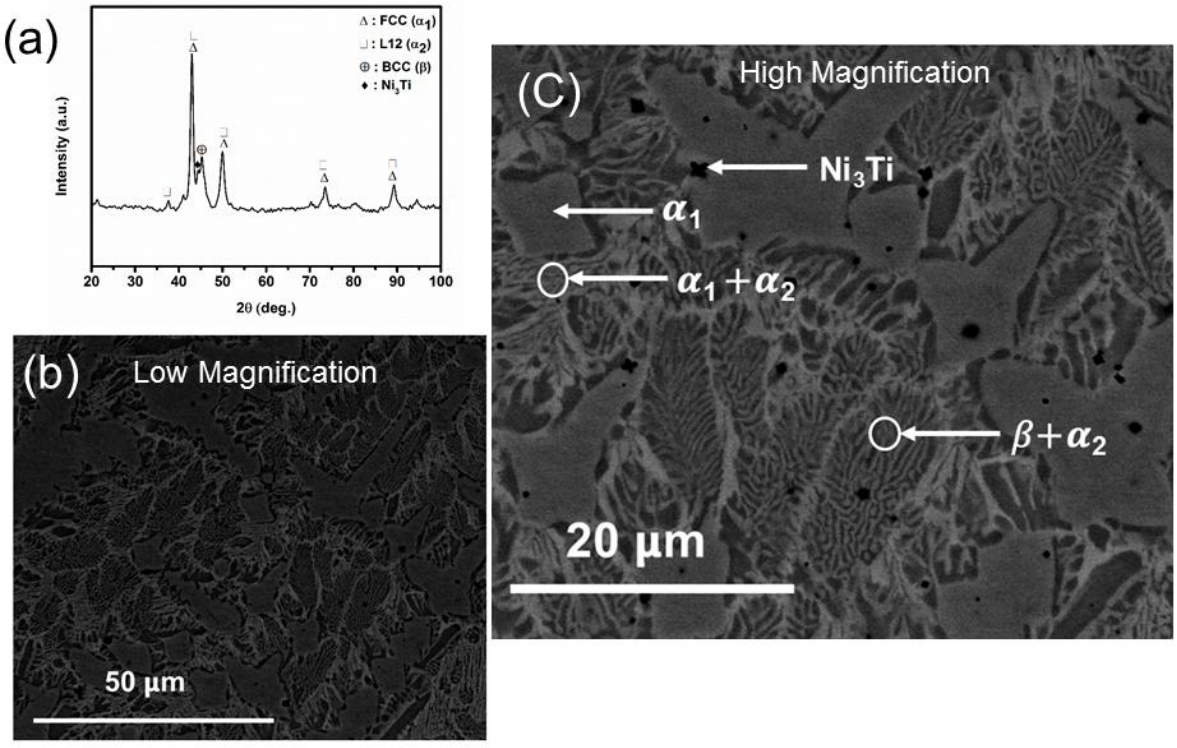

Figure 2: (a) XRD pattern, (b) and (c) SEM micrograph of multicomponent $Co_{25}Fe_{25}Ni_{25}Ti_{20}V_5$HEA.

3.3. Microstructural characterization

The detailed microstructural characterization of multicomponent EHEA was carried out using back scattered electron (BSE) imaging mode in SEM. However, the representative SEM micrograph of the studied HEA is given in Figure 2b(low magnification image) and Figure 2c (high magnification image) to decipher the different phases in the microstructure. The different phases in the microstructure of the studied HEA are marked based on the compositional analyses using SEM coupled with EDS.The compositional measurement of

each phases in microstructure has also been carried out using TEM coupled with EDS (as shown in Table 1).

Phases	Co	Fe	Ni	Ti	V
FCC (α_1)	24.20	24.30	22.20	24.40	4.90
FCC (α_2)	25.10	25.70	20.60	24.50	4.10
BCC (β)	29.90	30.60	9.90	23.80	5.90
Ni_3Ti	23.59	22.03	26.97	22.05	5.36

Table 1: EDS analysis of all the phases (composition in atomic percent) in microstructure of multicomponent $Co_{25}Fe_{25}Ni_{25}Ti_{20}V_5$ HEA.

The microstructure of multicomponentEHEA reveals the presence of primary $(Ni,Fe,Co)_3Ti$with black contrast, Ni-rich (i.e. Ni-Co-rich phase) solid solution phase with bright contrast (α_1) as well as light contrast (α_2) andNi-lean (i.e. Fe-Co-rich phase) solid solution phase gray contrast (β).

A detailed TEM characterization of the suction cast (ϕ = 6 mm) EHEAwas done to elucidate the fine scale microstructural features (shown in Figure 3). The phases in the microstructure are identified using the obtained selected area diffraction (SAD) patterns. The microstructure reveals the presence of two eutectics i.e. (i) one eutectic is between disorder FCC1 solid solution phase (α_1) and order FCC2 solid solution phase (α_2) and (ii) other one is between order FCC2 solid solution phase (α_2) and BCC (β) solid solution phase as well as two dendritic phases i.e. ordered Ni_3Ti_DO24 and disorder FCC1 solid solution phase (α_1). It is important to note that all the equilibrium phases predicted by thermodynamic simulation (Figure 1) except C14_LAVES phase are observed in the microstructure of the studied EHEA.

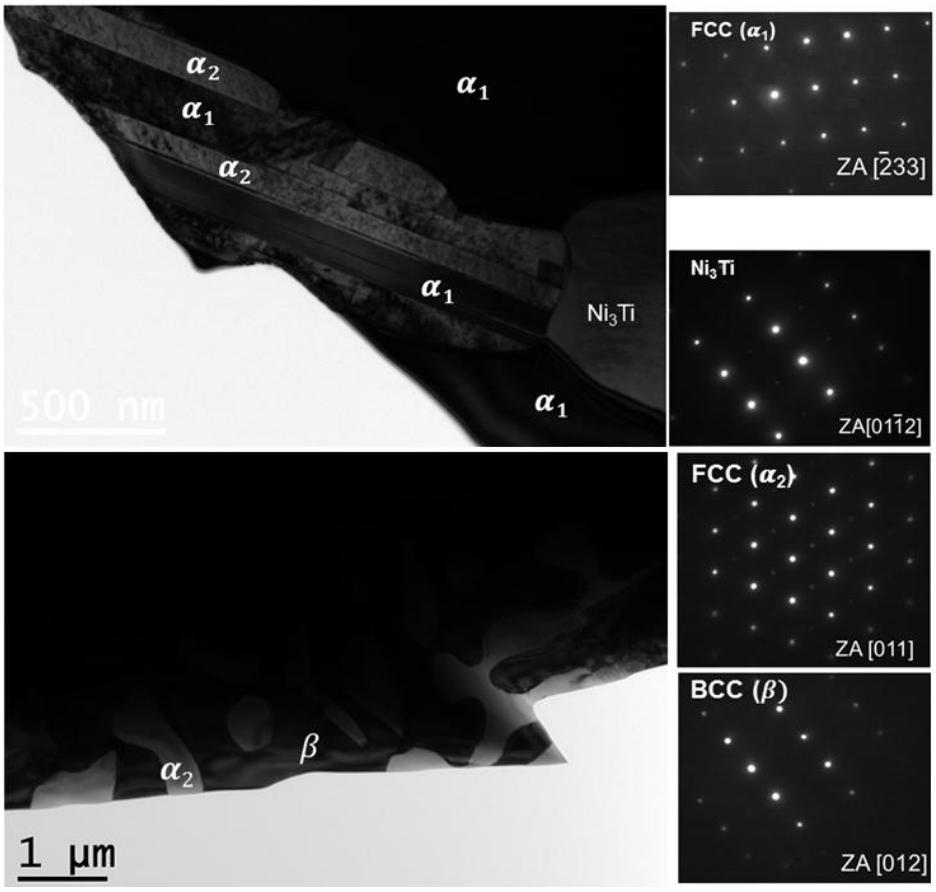

Figure 3: TEM micrograph of multicomponent $Co_{25}Fe_{25}Ni_{25}Ti_{20}V_5$HEA.

3.4. Phase equilibria in multicomponent $Co_{25}Fe_{25}Ni_{25}Ti_{20}V_5$HEA

It is important to note from microstructural characterization that there are one peritecticreaction i.e. Ni_3Ti + L⟶FCC_1(α_1) and two eutectics reactions i.e.coarse eutectic: L⟶disorder FCC_1 (α_1) + order FCC_2 (α_2) and fineeutectic: L⟶order FCC_2 (α_2) + BCC (β) features in the microstructure of studied HEA.

The solidification pathways for the investigated multicomponent EHEA has been described in the following;

(i) at first Ni_3Ti primary dendritic phase is evolved from the liquid during solidification, followed by

(ii) the peritectic reaction to form disorder FCC_1 solid solution phase FCC_1(α_1) i.e. Ni_3Ti + L⟶FCC_1(α_1)and then

(iii) the remaining liquid undergoes eutectic reaction to from disorder FCC_1 (α_1) and order FCC_2 (α_2)phases (i.e. coarse eutectic: L⟶FCC_1 (α_1) + FCC_2 (α_2)and

(iv) finally, the remaining liquidundergoes eutectic reaction to form order FCC_2 (α_2) and BCC (β) (i.e. fineeutectic: L⟶FCC_2 (α_2) + BCC (β)

Based upon the microstructural features observed in the studied multicomponent EHEA, the two different types of four phases reactions i.e. L+ Ni_3Ti → FCC_1 (α_1) + FCC_2 (α_2) and L+ FCC_1 (α_1) ⟶FCC_2 (α_2) + BCC (β) have been proposed for the investigated HEA. These four phase reactions are known as pseudo-quasiperitectic reactions. The first four phases reaction at point P1 is cooperated by two reactions i.e. Ni_3Ti + L⟶FCC_1(α_1) and L⟶FCC_1 (α_1) + FCC_2 (α_2) above and below point P1 respectively.Similarly, thesecond four phases reaction at point P2 is cooperated by two eutectic reactions i.e. L⟶FCC_1 (α_1) + FCC_2 (α_2) and L⟶FCC_2 (α_2) + BCC (β) above and below point P2 respectively.

3.5.Mechanical properties of $Co_{25}Fe_{25}Ni_{25}Ti_{20}V_5$HEA

The true stress-strain curves of the multicomponent EHEAat different temperatures (700^{o}C (973 K), (800^{o}C (1073 K), (900^{o}C (1173 K) and 1000^{o}C (1273 K) at a fixed strain rate of $10^{-1}s^{-1}$ were obtained for cylindrical samples (diameter (ϕ) = 6 mm and aspect ratio of 1.5:1). It is to be noted from Figure 4 that the flow stress decreases with increase in temperature at a constant strain rate of 10^{-1} s^{-1}.

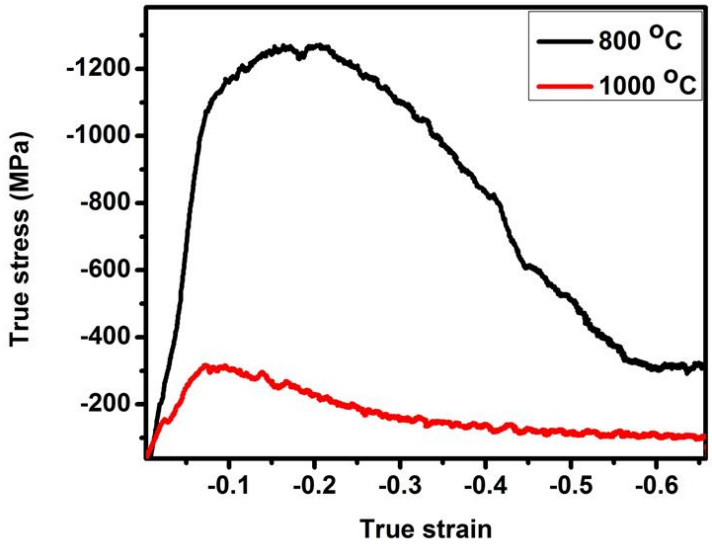

Figure 4:(a) True stress vs. strain curve of the multicomponent $Co_{25}Fe_{25}Ni_{25}Ti_{20}V_5$HEA at 800^{o}C, 1000^{o}C and strain rate of 10^{-1} s^{-1}.

It is also observed that after the reaching the yield stress, the studied alloy deforms plastically up to 65 % of true strain value with no fracture of the specimen. It is important to note that the high strength of the studied HEA at high temperature is attributed to the presence of unique composite microstructure i.e. bimodal eutectics at different length scale and peritectic morphology.One major finding of the present study is the presence of two different eutectics at different length scale in the designed multicomponent HEAs. Therefore, this type of unique microstructural features consisting of peritectic and bimodal eutecticsat different length scale observed in the studied multicomponent EHEA can be considered as potential candidate for high temperature structural applications.

4. Conclusions

Based on the results and discussion with respect to the present investigated multicomponent$Co_{25}Fe_{25}Ni_{25}Ti_{20}V_5$ HEA, the following conclusion can be drawn;

- The detailed sequence of phase evolution in the newly designed multicomponent HEAhas been understood by adopting experimental and thermodynamic simulation approach.
- The new phase equilibria i.e. Pseudo-quasiperitectic reactions have been proposed in the designed multicomponent HEA
- The high strength at elevated temperature is attributed to the unique microstructural features consisting of one peritectic and two types of eutectics in the microstructure.

References:

[1] J.W. Yeh, S.K. Chen, S.J. Lin, J.-Y. Gan, T.S. Chin, T.T. Shun, C.H. Tsau, S.Y. Chang, Adv. Eng. Mater. 6 (2004) 299–303.

[2] B. Cantor, I.T.H. Chang, P. Knight, A.J.B. Vincent, Mater. Sci. Eng. A. 375-377 (2004) 213–218.

[3] S. Mridha, S. Samal, P.Y. Khan, K. Biswas, Govind, Metall. Mater. Trans. A Phys. Metall. Mater. Sci. 44 (2013) 4532–4541.

[4] B.S. Murty, J.W. Yeh, S. Ranganthan, High Entropy Alloys, Elsevier, 2014.

[5] S. Guo, C. Ng, C.T. Liu, Mater. Res. Lett. 1 (2013) 228–232.

[6] Y. Zhang, T.T. Zuo, Z. Tang, M.C. Gao, K. A. Dahmen, P.K. Liaw, et al., Prog. Mater. Sci. 61 (2014) 1–93.

[7] S. Samal, S. Mohanty, A.K. Misra, K. Biswas, B. Govind, Mater. Sci. Forum. 790-791 (2014) 503–508.

[8] S. Mohanty, S. Samal, A. Tazuddin, C.S. Tiwary, N.P. Gurao, K. Biswas, Mater. Sci. Technol. 31 (2015) 1214–1222.
[9] K.Y. Tsai, M.H. Tsai, J.W. Yeh, Acta Mater. 61 (2013) 4887–4897.
[10] D.L. Beke, G. Erdélyi, Mater. Lett. 164 (2016) 111–113.
[11] O.N. Senkov, G.B. Wilks, J.M. Scott, D.B. Miracle, Intermetallics. 19 (2011) 698–706.
[12] A.K. Mishra, S. Samal, K. Biswas, Trans. Indian Inst. Met. 65 (2012) 725–730.
[13] S. Samal, Rahul MR, R. S. Kottada, G. Phanikumar, Mater. Sci. Eng. A, 664 (2016) 227–235, 2016.
[14]Rahul MR, S. Samal, S. Venugopal, G. Phanikumar, J. Alloys Compd., 749 (2018) 1115-1127